Spring 4-16-2018

A Review of the Seismic Isolation Design Procedure

Francisco Garcia
University of Nebraska-Lincoln

A Review of the Seismic Isolation Design Procedure

An Undergraduate Honors Thesis

Submitted in Partial fulfillment of

University Honors Program Requirements

University of Nebraska-Lincoln

by

Francisco Garcia, BS

Civil Engineering

College of Engineering

March 2018

Faculty Members:

Dr. Joshua S. Steelman, PHD, Civil Engineering

Abstract

The current design procedure for seismic isolation bearings for bridges is a simplified method that assigns the bearings with an elastic stiffness. Bridges subjected to ground motions actually act in a hysteric, nonlinear fashion when force is plotted against displacement. The goal of this research was to gain further insight as to whether simplifying seismic isolation bearings to a simplified stiffness is adequate or not. Design procedures were followed in the modeling of a bridge with seismic isolation. Linear modal time history analyses and with nonlinear direct integration time history analyses of ground motions were compared. At the conclusion of this study, it is still unclear as to whether the simplification of the bearings' motions that are used in contemporary bridge design were adequate or not. It should be noted that structural modeling methods are very sensitive that require rigorous and complex calculations to check. Additional work would be required on the bridge model developed in order to determine whether the current design standards for seismic isolators are adequate.

Keywords: seismic isolation design, elastomeric bearing, bridge engineering, bridge modeling, civil engineering

Acknowledgements

This project could not have been done without the love, support, and encouragement of many people I am blessed to have in my life. The first people I would like to acknowledge are my parents. They are the hardest working people that I have ever known and without them I would certainly not be where I am today. They have sacrificed so much to see me succeed. They have believed in me when I didn't believe in myself.

I would also like to extend gratitude to Dr. Joshua S. Steelman. Thanks for being an excellent teacher and for brilliantly introducing me to structural engineering in the class I had with you nearly two years ago. I would also like to thank him for taking a chance on undergraduate researchers this past year. I have learned about structural dynamics, SAP2000, and my interest in structural engineering has grown since we started working together. Thank you again for all of the late nights that you invested into this work.

I would also like to thank the Department of Civil Engineering at UNL and all of the students that have welcomed me into their lives. I am privileged to have learned from engaging professors alongside passionate students.

Finally, I would like to thank all of my friends. Thanks to the Society of Hispanic Professional Engineers and my staff at Kauffman for being patient and flexible with my last crazy semester. Thank you Anna for being so supportive and encouraging throughout this project. Thanks to all of the friends I have made along the way at Kauffman, the shire, ODK, and the soccer field. All of you have contributed to my success and I am grateful for you being a part of my life. I could go on and on with how blessed I am to have you and others I did not specifically mention, but the show has to start now.

A Review of the Seismic Isolation Design Procedure

Introduction

Isolation refers to a strategy of introducing flexible elements between the ground and a structure, reducing the transmissibility of seismic ground motion to and corresponding inertial loads in the structure. While isolation seems to provide superior performance, common design procedures have also been greatly simplified to facilitate use in practice. Safety is ensured in structural design through consideration of probabilistic combinations of hazard sources and intensities, but the deterministic formulations mask the true variability expected in structural behavior and performance, particularly for earthquakes. In modern bridge design specifications (AASHTO, 2017), seismic demands are considered in the Extreme Event I load combination, and are commonly addressed using Equivalent Lateral Force (ELF) approaches. ELF procedures treat seismic loads as equivalent static loads, but seismically induced demands are highly dynamic. Acceptable designs meeting code-specified requirements (typically satisfied through ELFs) only ensure that bridges do not collapse during major earthquakes. However, supplementary discrete thresholds of damage may also be required by bridge owners corresponding to a range of earthquake severity levels (Marsh and Stringer, 2013).

Furthermore, seismic isolation reduces damage and downtime for structures. There was a 6.7 magnitude earthquake in Northridge, CA in 1994 that cost $20 billion in damages to 31 Los Angeles area hospitals (Mayes, 2012). On top of that, nine of the hospitals had to evacuate. The only hospital that faced no damage at all was the USC Hospital which had a base isolation system installed. A km away, the Los Angeles County General Hospital sustained $389 million in damages.

The Kobe, Japan 7.1 magnitude earthquake of 1995 caused $150 billion (Mayes, 2012). Despite the earthquake's severity, the world's largest base-isolated computer center, a 6-story, reinforced concrete building, suffered no damages. A similar 6-story, non-isolated, reinforced concrete building on an adjacent block serves as great way of analyzing the impact the isolation system had. The non-isolated building amplified the ground motions by a factor of 3 at the roof as opposed to the isolated building which actually reduced ground motions by a factor of 10 at the roof.

The 4th edition of the American Association of State Highway and Transportation Officials (AASHTO) Guide Specifications for Seismic Isolation Design (GSSID) outlines a design process wherein seismic isolation bridge bearings are placed between the substructure (piers and foundations) and the superstructure (girders and roadway deck) of a bridge (AASHTO GSSID, 2014) . The bearings that were studied are lead rubber bearings, a subset of elastomeric bearing isolators available in practice.

Each bearing physically consists of a dense lead core surrounded by steel-reinforced rubber. A thick steel plate is bonded to the rubber at the top and bottom surfaces to enable positive connection to super- and substructure elements. This type of isolation bearing is relatively common in bridge isolation design. A design stiffness is determined which is then used to proportion the size and dimensions of the lead core, steel plates, and the rubber with steel reinforcement. Elastomeric bearings can be designed to be rectangular or circular.

The bearings offer flexibility in the transverse and longitudinal directions by deforming due to shear so that the superstructure and substructure experience large relative deformations, yet do not physically break off from each other. The idea of isolation systems is that they are 'isolated' from the ground motion so that bridges can survive earthquakes by reducing

transmissibility of ground motions from sub- to superstructure and therefore reducing inertial force demands.

Work by Dr. Ian Buckle of the University of Nevada, Reno was reviewed extensively. Buckle is a prominent researcher in bridge isolation and has contributed extensively to the AASHTO GSSID, including the development of a suite of detailed, parametric design examples. The examples portray design procedures for two benchmark bridges. The first benchmark bridge is a short-span concrete bridge, and the second is a long-span steel bridge. Six variations of the two bridges were considered with various seismic hazards, site classes, pier heights, skew, and isolator types. Isolator types included lead-rubber bearings, spherical friction bearings (friction pendulum bearings), and Eradiquake bearings. Spherical friction bearings work by allowing the structure above the bearing to slide during an earthquake on a low friction, curved surface.

Buckle, Moustafa Al-Ani, and Eric Monzon illustrated the design methodology for seismic isolation bearings in a presentation for the Technical Subcommittee for Bearings and Expansion Devices at the Annual AASHTO subcommittee meeting on bridges and structures (Buckle et al., 2012). The general isolation system design procedure begins with assembling bridge and site data. Performance objectives also have to be defined. Next, the bridge is analyzed in the longitudinal direction. This step can be done by using a simplified method or a multi-modal spectral analysis method. After that, the bridge is analyzed in the transverse direction with the simplified or multi-modal method. The results are combined and the performance of the bridge is checked. Finally, the physical bearing properties can be designed for.

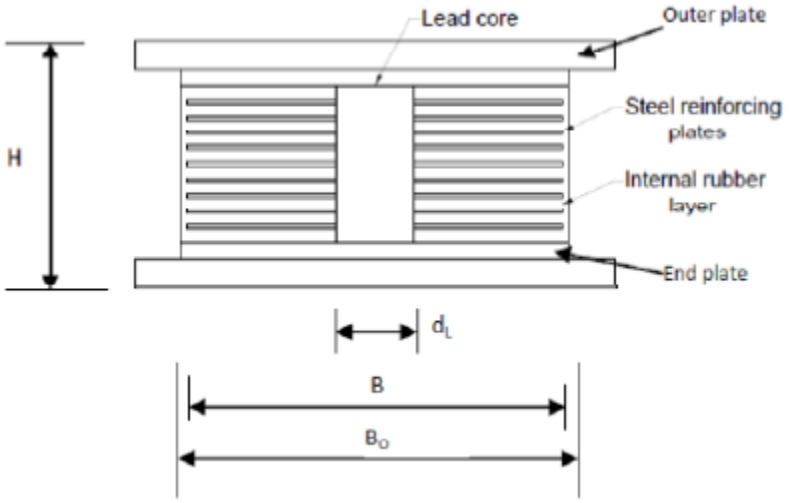

Figure 1. Elastomeric Bearing

Review of AASHTO GSSID

The 4th edition of the AASHTO GSSID is reflective of the research and work that Dr. Buckle does. This edition was published in 2014 and has few design example for engineers to reference when designing isolation systems. The example that was primarily examined in this review is called Benchmark Bridge No. 2 (Example 2). This example is described by Dr. Buckle,

"Benchmark bridge No. 2 is a straight, 3-span, steel plate-girder structure with single column piers and seat-type abutments. The spans are continuous over the piers with span lengths of 105 ft, 152.5 ft, and 105 ft for a total length of 362.5 ft (Figure 2.1). The girders are spaced 11.25 ft apart with 3.75 ft overhangs for a total width of 30 ft. The built-up girders are composed of 1.625 in by 22.5 in top and bottom flange plates and 0.9375 in. by 65 in. web plate. The reinforced concrete deck slab is 8.125 in thick with 1.875 in. haunch. The support and intermediate cross-frames are of V-type configuration as shown in Figure 2.2. Cross-frame spacing is about 15 ft throughout the bridge length. The total weight of superstructure is 1,651 kips. All the piers are single concrete columns with a diameter of 48 in, longitudinal steel ratio of 1%, and transverse steel ratio of 1%. The calculated plastic moment is equal to 3,078 kft and the plastic shear (in single curvature) is 128k. The total height of the superstructure is 24 ft above the ground. The clear height of the column is 19ft. The design of an isolation system for this bridge is given in this section, assuming the bridge is located on a rock site where the PGA = 0.4, S_S = 0.75 and S_1 = 0.20. A 2-column format is used for this design example… (p.269)."

The first step to the design process is to assemble the bridge and site data. The example problem does so by calculating the weight of superstructure per support, determining the pier stiffnesses assuming a fixed footing, and assembles a design response spectrum in accordance with GSSID and LRFD specifications. The pier stiffness, $k_{sub,pier}$, was calculated to be different than that in the GSID. . After the bridge was modeled using SAP2000 structures modeling software, a lower value was found. Unfortunately, the GSSID does not mention how this value calculated.

The model was checked using different methods. First, a vertical stiffness check was used. A simplified model was developed by calculating the weight of the model per foot in the

longitudinal direction. This model is a two dimensional model that was only used to test the validity of the one already made. A load was applied to both bridges in the middle and the

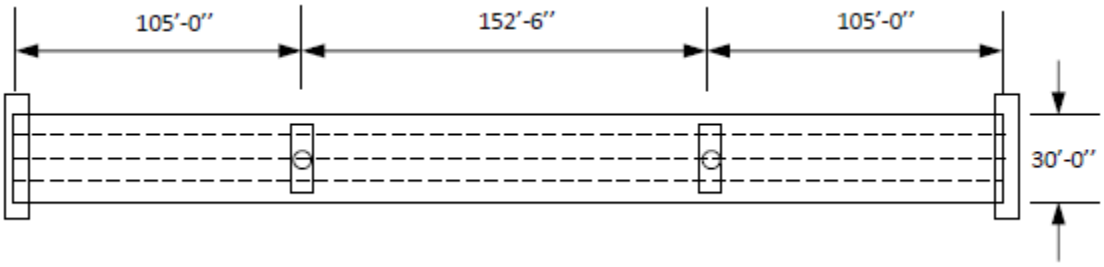

Figure 2. Map View of Benchmark No. 2

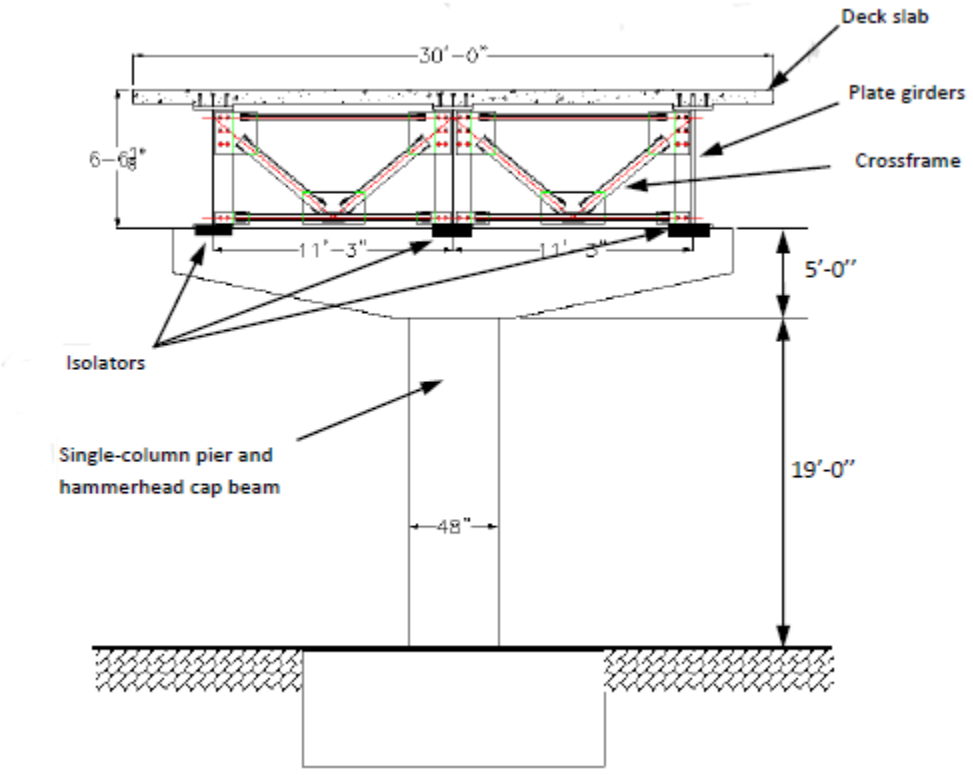

Figure 3. Cross-Section View of Benchmark No. 2

displacement was found to be the same. This means that everything in the gravity direction was acting as expected. Next, a series of calculations were performed to try to validate the k_{sub}

calculated in the GSSID which is 288.87 kips per inch. Once none of the methods were able to validated with the GSSID's pier stiffness, researchers were contacted with some of the following calculation details.

Method 1: Back-calculate stiffness corresponding to a stated structural dynamic period.

Recalling single degree-of-freedom dynamics, the undamped angular natural frequency, ω_n, is related to stiffness, k, and mass, m, using:

$$\omega_n = \sqrt{\frac{k}{m}} \tag{1}$$

Angular and regular natural frequency, f, are related by:

$$\omega_n = 2\pi f \tag{2}$$

And regular natural frequency is the reciprocal of natural period, T:

$$f = \frac{1}{T} \tag{3}$$

Substituting and rearranging terms:

$$k = \left(\frac{2\pi}{T}\right)^2 * m \tag{4}$$

A natural period, T, equal to 1.463 seconds is given in the GSSID example documentation for longitudinal translation (B3.1.2.2.6, Step B2.6). The weight of the superstructure is given as 1,651 kips, and the participating weight of the piers for purposes of period calculation is 256 kips. The total weight, W, for period calculations is approximately 1908 kips (B3.1.1.1, Step A1). To avoid any potential confusion associated with force and mass in United States customary units, subsequent calculations will be performed in SI units:

$$W = 1908\ kips * \frac{4448\ N}{1\ kip} = 8.487 * 10^6\ N = 8.487 * 10^6\ \frac{kg * m}{sec^2} \tag{5}$$

Dividing weight by gravitational acceleration to obtain mass, m, in *kg*:

$$m = 8.487 * 10^6\ \frac{kg * meter}{sec^2} * \frac{sec^2}{9.81\ meters} = 8.651 * 10^5\ kg \tag{6}$$

Substituting the mass from Equation (6) and the stated period, T, for longitudinal motion into Equation (4):

$$k = \left(\frac{2\pi}{1.463\ sec}\right)^2 * 8.651 * \ 10^5\ kg = 1.596 * \ 10^7\ \frac{kg}{sec^2} \tag{7}$$

Finally, converting back to United States customary units to obtain the effective system stiffness:

$$k = 1.596 * 10^7\ \frac{N}{m} * \frac{1\ kips}{4448\ N} * \ \frac{0.0254\ m}{1\ in} = 91.14\ \frac{kips}{in} \tag{8}$$

Alternatively, considering an equivalent viscous damping ratio of 30% as noted in B3.1.2.1.10 (Step B1.10) and Table B3.1.2.1.12-1, the damped and undamped angular natural frequencies are related using:

$$\omega_D = \omega_n\sqrt{1-\zeta^2} \tag{9}$$

And the damped period becomes:

$$T_D = \ \frac{2\pi}{\omega_n\sqrt{1-\zeta^2}} \tag{10}$$

So, the stiffness accounting for damping becomes:

$$k_D = m\left(\frac{2\pi}{T_D}\right)^2 \frac{1}{(1-\zeta^2)} \tag{11}$$

$$k_D = 8.651 * \ 10^5\ kg\left(\frac{2\pi}{1.463\ s}\right)^2 \frac{1}{(1-0.3^2)} = 1.753 * 10^7\ \frac{N}{m} \tag{12}$$

$$k_D = 1.753 * 10^7\ \frac{N}{m} * \frac{1\ kips}{4448\ N} * \ \frac{0.0254\ m}{1\ in} = 100.10\ \frac{kips}{in} \tag{13}$$

For substructures acting as parallel springs, using GSSID Eq. (7.1-6) (B3.1.2.1.4, Step B1.4):

$$(k\ or\ k_D) = K_{eff} = \sum_{j=1}^{m\ substructures} K_{eff,j} \tag{14}$$

The GSSID presents Eq. (7.1-7) to characterize the series stiffness of the pier, k_{sub}, and the isolators, k_{eff}, with an effective individual substructure stiffness, $K_{eff,j}$ (note: the j subscript has

been maintained throughout all terms, although it is omitted on the right side of the equation in the GSSID):

$$K_{eff,j} = \frac{k_{sub,j} * k_{eff,j}}{k_{sub,j} + k_{eff,j}} \tag{15}$$

The k_{eff} term represents the stiffness of all isolators at a substructure unit, so, at each pier or abutment:

$$k_{eff,j} = K_{isol,j} = \sum K_{isol,i} \tag{16}$$

Because the piers are identical and the abutments are identical:

$$(k \; or \; k_D) = K_{eff} = 2 * K_{eff,pier} + 2 * K_{eff,abut} \tag{17}$$

$$K_{eff,pier} = \frac{(k \; or \; k_D)}{2} - K_{eff,abut} \tag{18}$$

According to Table B3.1.2.1.12-1, the abutment substructure stiffness, $k_{sub,abut}$, was assumed to be approximately 10,000 kips / in. The total stiffness of the isolators, $\sum K_{isol,abut}$, is listed under $K_{isol,j}$ in the same table, as 10.216 kips / in.

$$K_{eff,abut} = \frac{k_{sub,abut} * \sum K_{isol,abut}}{k_{sub,abut} + \sum K_{isol,abut}} = \frac{10{,}000 \; \frac{kip}{in} * 10.216 \frac{kip}{in}}{10{,}000 \; \frac{kip}{in} + 10.216 \frac{kip}{in}} = 10.21 \; \frac{kip}{in} \tag{19}$$

So, using undamped stiffness, k,

$$K_{eff,pier} = \frac{91.14 \frac{kip}{in}}{2} - 10.21 \; \frac{kip}{in} = 35.36 \frac{kip}{in} \tag{20}$$

And

$$K_{eff,pier} = 35.36 \frac{kip}{in} = \frac{k_{sub,pier} * \sum K_{isol,pier}}{k_{sub,pier} + \sum K_{isol,pier}} \tag{21}$$

Finally, with $\sum K_{isol,pier}$ taken as 42.778 kips / in (again from Table B3.1.2.1.12-1),

$$k_{sub,pier} = \frac{K_{eff,pier}}{\left(1 - \frac{K_{eff,pier}}{\sum K_{isol,pier}}\right)} = \frac{35.36\frac{kip}{in}}{\left(1 - \frac{35.36\frac{kip}{in}}{42.778\frac{kip}{in}}\right)} = 204\frac{kip}{in} \quad (22)$$

This value is 28% lower than the published pier substructure stiffness, 288.87 kips / in.

If the damped stiffness is used (substituting the value of 100.10 kips / in obtained in Equation (13) into Equation (20)), instead of the undamped stiffness (91.14 kips / in obtained in Equation (8)), the pier stiffness is determined to be 581.4 kips / in, 101% higher than the published value.

If a commonly assumed value of 5% damping is used, matching the value typically associated with ground motion hazard maps, the pier stiffness is estimated to be 207.9 kips / in, 28% lower than the published value.

The substructure stiffness inferred using the structural period could not be brought into agreement with the substructure stiffnesses documented in the GSSID Example No. 2. The inferred values enveloped the published values, depending on the level of damping used for the calculations.

Method 2: Directly calculate pier stiffness from fundamental mechanics.

This method analyzes the pier as a vertical cantilever beam, with a fixed end at the base. The pier is assumed to have no or negligible rotational or translational restraint at the top. Loading consists of a concentrated shear load corresponding to superstructure inertia during seismic excitation (horizontal and parallel to the superstructure span direction). The assumption of a true cantilever is believed to be consistent with the GSSID example, which indicates only translational stiffness quantities for the bearings. The stiffness of a cantilever beam with cross-section flexural rigidity EI and length L, loaded with a concentrated force at the free end, is known from fundamental mechanics to be

$$k_{sub,pier} = \frac{3EI}{L^3} \quad (23)$$

The modulus of elasticity for concrete can be estimated using guidance available from ACI 318. However, doing so requires knowledge of concrete strength. The concrete strength was not found in the example documentation. The concrete strength was assumed to be 4,000 psi. The modulus of elasticity was then estimated to be

$$E = 57{,}000\sqrt{f'_c} = \frac{57{,}000\sqrt{4{,}000\ psi}\ (psi)}{1000\ psi}\ ksi = 3{,}605\ ksi \tag{24}$$

The moment of inertia, I, is determined from dimensions provided in the example. The pier is composed of a circular column 4 ft in diameter and 19 ft tall (clear height to the bottom of the cap), topped by a hammerhead cap approximately 22.5 ft wide, 4 ft long, and 5 ft tall. For the gross circular section,

$$I_{gross} = \frac{\pi D^4}{64} = \frac{\pi\left(4\ ft * \frac{12\ in}{1\ ft} = 48in\right)^4}{64} = 260{,}600\ in^4 \tag{25}$$

The example documentation states in B3.1.1.1, with regard to substructure stiffness: "The calculation of these quantities requires careful consideration of several factors, such as the use of cracked sections when estimating column or wall flexural stiffness, foundation flexibility, and effective column height." Foundation flexibility is disregarded, and the foundation is assumed to be infinitely rigid against rotation, because no details of the soil conditions or foundation design were found in the example documentation. The example does not specifically state whether cracked section properties were used, but the quoted text suggests that pier substructures may have considered cracked stiffness. ACI 318 suggests that only 70% of column moment of inertia should be considered effective to reflect a loss of stiffness associated with cracking.

Lastly, the example documentation mentions "effective column height". It is unclear whether the full height, including the cap, was included in the substructure stiffnesses. Four options were therefore considered for validation calculations:

- Option 1: L = 19 ft (ignore cap), I = I_{gross}
- Option 2: L = 19 ft (ignore cap), I = $I_{cracked}$ = 70% of I_{gross}
- Option 3: L = 24 ft (include cap), I = $I_{cracked}$ = 70% of I_{gross} constant for the full height (neglect increased moment of inertia through cap height)
- Option 4: L = 24 ft (include cap), I = I_{gross} for the circular portion of the height, I assumed practically infinite at the cap

For Option 1:

$$k_{sub,pier} = \frac{3(3605\ ksi)(260600\ in^4)}{(19 * 12\ in)^3} = 237\ kip/in \tag{26}$$

For Option 2:

$$k_{sub,pier} = \frac{3(3605\ ksi)(0.7 * 260600\ in^4)}{(19 * 12\ in)^3} = 166\ kip/in \quad (27)$$

For Option 3:

$$k_{sub,pier} = \frac{3(3605\ ksi)(0.7 * 260600\ in^4)}{(24 * 12\ in)^3} = 82.5\ kip/in \quad (28)$$

For Option 4:

First, the deformation at the top of the 19 ft segment was evaluated. The full uncracked moment of inertia was assumed to be effective (as in Equation (26), above). A unit load at the top of the cap will effectively impose a unit shear and a 5 k-ft moment (1 kip * 5 ft hammerhead cap height) at the top of the 19 ft segment. The deflections from these load effects will be 4.206 x 10^{-3} inches and 1.660 x 10^{-3} inches, respectively, at the top of the 19 ft segment. The rotations will be 2.767 x 10^{-5} radians and 1.456 x 10^{-5} radians, respectively. Summing the rotations and multiplying by the (5 ft = 60 inches) hammerhead height produces an additional 2.534 x 10^{-3} inches of deformation at the top of the cap relative to the top of the 19 ft segment, using small angle theory and assuming the cap to be a rigid block undergoing a rotation. Combining this additional displacement with the sum of the displacements from the concentrated load and moment at the top of the 19 ft. segment results in a total displacement of 8.40 x 10^{-3} inches of total deformation at the top of the cap as a result of a 1 kip load. Therefore,

$$k_{sub,pier} = \frac{1\ kip}{8.40 * 10^{-3}\ in} = 119.0\ kip/in \quad (29)$$

In summary, the documented substructure stiffnesses could not be replicated using fundamental mechanics. All cases considered produced stiffness estimates lower than the published values provided in the example documentation. The value obtained using only the 19 ft height and the full uncracked moment of inertia would seem to be an unrealistic option, yet it provided the closest value to those published in the example documentation. The calculated pier substructure stiffnesses, relative to the stated value in the example, were:

- Option 1: 18% lower
- Option 2: 43% lower
- Option 3: 71% lower
- Option 4: 59% lower

Fortunately, the researchers were able to address the discrepancies our calculations claim. The ACI estimate for concrete compressive strength was not the same. Dr. Buckle used an expected concrete strength of 5.5 kips per square inch instead of 4 kips per square inch. Once this value is used, we can calculate a different concrete modulus of elasticity using an equation for modulus of elasticity. This formula comes from the AASHTO LRFD specifications, not ACI. The value they calculated the compressive strength to be is 4,496 kips per square inch.

$$E_c = 33{,}000\ {w_c}^{1.5}\sqrt{f'_c} = 33{,}000\ (0.150\ kips/feet^3)^{1.5}\sqrt{5.5\ ksi} = 4{,}496\ ksi$$

Assuming a pier length of 19 ft. with uncracked section properties, the researchers found the stiffness value that is in the GSSID by using equation 26.

$$k_{sub,pier} = \frac{3(4496\ ksi)(260600\ in^4)}{(19 * 12\ in)^3} = 288.87\ kip/in$$

The validity of this number should be checked for two reason. One reason that this may be wrong is because the researchers assume that the pier height is 19ft. This assumption neglects all of the stiffness the pier cap has. This assumption should not be taken lightly since this is taken to the third power in equation 26. Neglecting the five feet could affect the pier stiffness significantly. Furthermore, the researchers assumed that the effective moment of inertia of the column is 100% of the gross moment of inertia. Factors usually reduce the effective moment of inertia because of cracking. ACI for example allows for the effective moment of inertia to be 70% of the gross moment of inertia for columns.

The next step of the design procedure is to determine the isolator stiffness, k_{isol}, based on bilinear isolator properties. This can be done with a simplified method that was verified. Since the force is dependent on the displacement, the process is iterative and can be solved with a

spreadsheet program. A summary of how k_{isol} is described below. Buckle claims that using k_{isol} is an adequate representation of the bearing's hysteric motion.

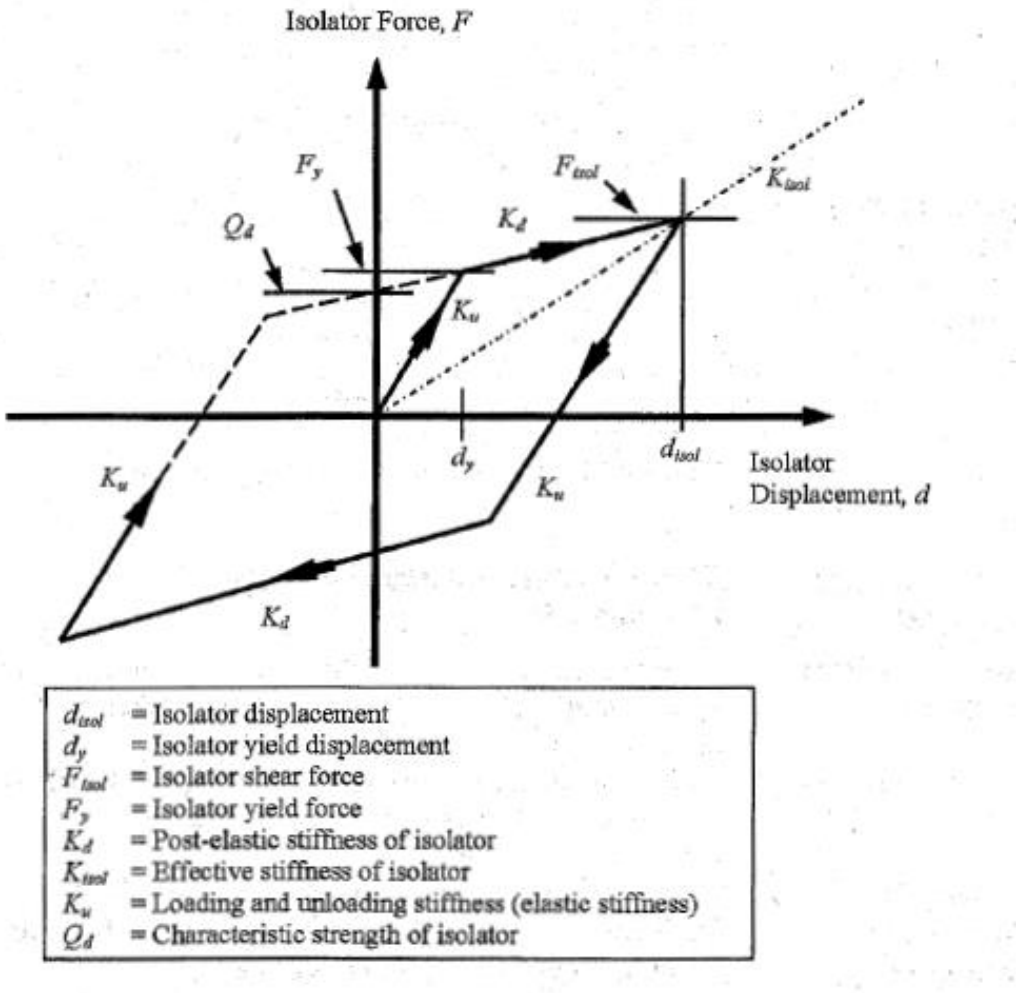

Figure 4. Properties of Bilinear Isolators

In B3 .1.2.1.1-2 of the GSSID, Q_d is taken to be five percent of the bridge weight.

$$Q_d = 0.05 * W = 0.05 * 1651.32\ kips = 82.56\ kips$$

Equation B3.1.2.1.1-3 sets the minimum post-yield stiffness, k_d. The researchers claim that a good place to start is twice the minimum value. An initial displacement of 2 inches is assumed to begin the iterative process.

$$K_d \geq \frac{0.025W}{d}$$

$$K_d = \frac{0.05W}{d} = \frac{0.05 * 1651.32\ kips}{in} = 41.28\ {}^{kips}/_{in}$$

Q_d and K_d reflect the entire isolation system. They can be divided into individual pier and abutments by multiplying them by the ratio of the weight that the pier or abutment supports over the entire superstructure weight. These are equations B3.1.2.1.2-1 and B3.1.2.1.2-2.

$$Q_{d,j}=Q_d \frac{W_j}{W}$$

$$K_{d,j}=K_d \frac{W_j}{W}$$

Next, the effective stiffness for each support is calculated by using equation B3.1.2.1.3-1:

$$K_{eff,j} = \frac{\alpha_j * k_{sub,j}}{1 + \alpha_j}$$

Where, α_j is given by equation B3.1.2.1.3-2:

$$\alpha_j = \frac{K_{d,j}d + Q_{d,j}}{k_{sub,j}d - Q_{d,j}}$$

Isolator displacement is calculated as such in B3.1.2..1.5-1

$$d_{isol} = \frac{d}{1 + \alpha_j}$$

It should be noted that $k_{sub,j}$ is taken as a large number, 10,000 kips per inch, at the abutments since it is very stiff there. $k_{sub,j}$ is taken to be 288.87 kips per inch which, as noted earlier, may not be as valid as the researchers assumed. Now, the effective period, T_{eff}, is calculated by using equation B3.1.2.1.10-1.

$$T_{eff} = 2\pi\sqrt{\frac{W_{eff}}{g\sum K_{eff,j}}} = 2\pi\sqrt{\frac{1907.58}{386.4 * 79.02}} = 1.57\ s$$

Using a damping factor of 30%, the displacement can be calculated using equation B3.1.2.1.11-2:

$$d = \frac{9.79 S_{D1} T_{eff}}{B_L} = \frac{9.79 * 0.2 * 1.57}{1.7} = 1.81\ in$$

Since the displacement calculated is not the same as our initial assumption (two inches), the iterative process is done again by using an initial displacement of 1.81 inches. The iteration converges to 1.65 inch displacement after three iterations. The GSSID recommends spreadsheet usage for this iterative procedure.

At the end of the iterative process, $Q_d = 2.81\ kips$, $K_d = 1.70\ {}^{kips}/_{in}$, $K_{isol} = 3.36\ {}^{kips}/_{in}$, and $d_{isol} = 1.66\ in$ for the isolators at the abutments. K_u was determined by using equation B3.1.2.2.2-1.

$$K_u = 10 * K_d = 10 * 1.70\ {}^{kips}/_{in} = 10.70\ {}^{kips}/_{in}$$

Equation B3.1.2.2.2-2 provides the yield displacement of the isolator.

$$d_y = \frac{Q_d}{K_u - K_d} = \frac{2.81}{17 - 1.7} = 0.18\ in$$

The isolator yield force can be calculated using simple graph relationships.

$$F_{isol} = Q_d + K_d(d_{isol} - d_y) = 2.81\ kips + \left(1.7\ {}^{kips}/_{in}\right)(1.66\ in) = 5.63\ kips$$

Dividing the isolator yield force by the isolator displacement then gives provides the isolator stiffness.

$$k_{isol} = \frac{F_{isol}}{d_{isol}} = \frac{5.63\ kips}{1.66\ in} = 3.4\ {}^{kips}/_{in}$$

This stiffness corresponds with what the researchers included in the GSSID. The process can be done for the pier columns to get an isolator stiffness of 15.8 kips per inch.

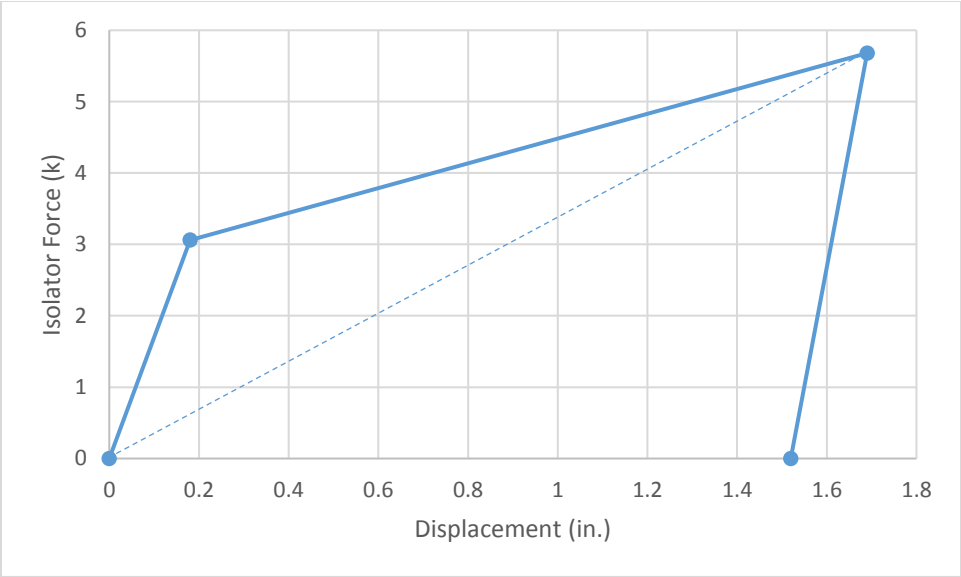

Figure 5. Isolator Properties for Abutments

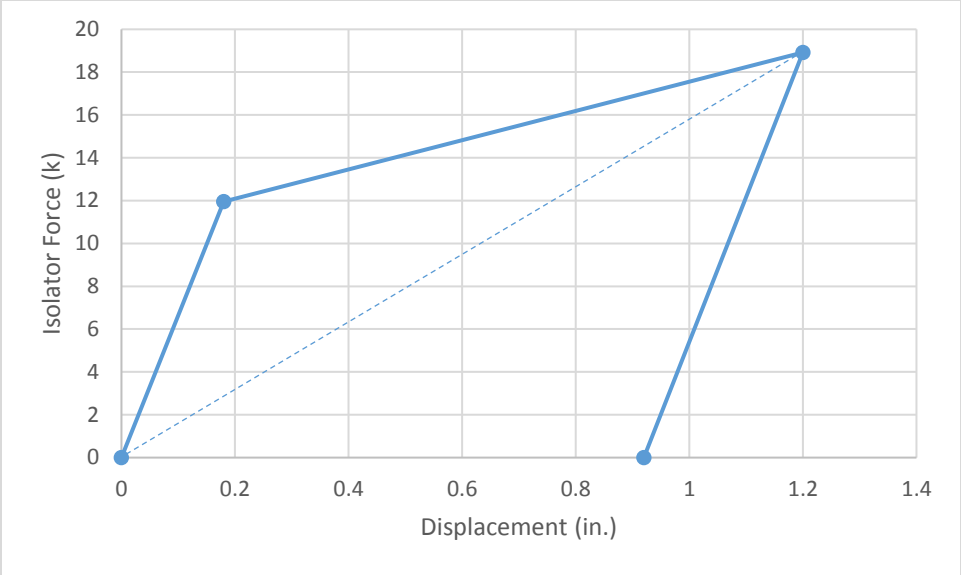

Figure 6. Isolator Properties for Piers Columns

The bridge model was subjected to modal analysis and compared to the modes that Buckle calculated. The first mode is 1.604 seconds that has a high mass participation ratio in the transverse direction. The second mode is 1.463 that has a high modal participation ratio in the longitudinal direction. The mode with longitudinal motion is the one that was considered the most in our analyses. The model was developed with spring stiffnesses equal to k_{isol} values for abutments and piers. The model prepared had a transverse mode of 1.27 seconds which is off of our expected value by about 0.16 seconds. The model's discrepancies can be attributed to differences in bridge models since some assumptions had to be when making the bridge model.

Nonlinear analysis was performed on the bridge model. One joint links took the place of three springs acting as the isolators at the abutments and two joint links replaced the individual springs at the piers. The same k_{isol} values for abutments and piers were entered to ensure that the model is still representative of how the bridge should behave. The modal analysis period in the longitudinal direction was less than a second off of the longitudinal mode of the model with

springs. The links were then altered to account for the hysteric motion that is expected to realistically happen during ground motions. Nonlinear direct integration time history was ran for scaled ground motions that were obtained from Pacific Earthquake Engineering Research Center (PEER) (Ancheta et al., 2013) in accordance with the work of Francys Mosquera (Mosquera, 2017). Peak displacements and corresponding forces were obtained for the piers and abutments from the model's analysis. Peak displacements and corresponding forces at the two locations for linear modal analysis was also performed to be compared to the nonlinear analysis data.

Results

Table 1. Peak Positive Displacement and Peak Force at Abutments (inches, kips)

	Analysis Type	
	Nonlinear	Linear Analysis
Ground Motion ID	Direct Integration	Modal
225 Brawley Airport	0.235, 3.155	0.366, 3.439
315 Brawley Airport	0.330, 3.32	0.337, 3.452
106 Canoga Park	0.195, 3.086	0.361, 3.694
196 Canoga Park	0.695, 3.954	0.577, 5.907
000 Capitola	0.183, 3.066	0.190, 1.940
090 Capitola	0.206, 3.104	0.107, 1.091
000 Fortuna	0.744, 4.309	2.347, 24.01
090 Fortuna	0.435, 3.503	1.058, 10.83
177 Glendale	0.155, 2.642	0.236, 2.411
267 Glendale	0.332, 3.323	0.300, 3.069
045 Plaster City	0.278, 3.231	0.240, 2.452
135 Plaster City	0.260, 3.199	0.261, 2.666
000 El Centro	0.619, 3.822	0.248, 2.540
090 El Centro	0.772, 4.087	0.863, 8.832

Table 2. Peak Positive Displacement and Peak Force at Piers (inches, kips)

	Analysis Type	
	Nonlinear	Linear Analysis
Ground Motion ID	Direct Integration	Modal
225 Brawley Airport	0.147, 11.72	0.315, 4.489
315 Brawley Airport	0.299, 12.76	0.318, 4.534
106 Canoga Park	0.226, 12.26	0.335, 4.774
196 Canoga Park	0.652, 15.17	0.542, 7.721
000 Capitola	0.157, 10.44	0.179, 2.549
090 Capitola	0.197, 12.07	0.100, 1.429
000 Fortuna	0.748, 15.83	2.194, 31.29
090 Fortuna	0.408, 13.50	0.987, 14.08
177 Glendale	0.169, 11.21	0.220, 3.137
267 Glendale	0.307, 12.81	0.280, 3.992
045 Plaster City	0.360, 13.18	0.223, 3.176
135 Plaster City	0.288, 12.69	0.245, 3.488
000 El Centro	0.621, 14.96	0.232, 3.312
090 El Centro	0.780, 16.05	0.806, 11.50

As we can see from the pier and abutment bearing displacements and forces from the tables, the linear analysis does not perfectly capture the movements we would expect to see in a nonlinear analysis. One example that the linear analysis does not capture the expected reactions is in 000 Fortuna. In the abutments, linear analysis yielded a force nearly six times higher than that of nonlinear analysis and a displacement more than triple that of the nonlinear analysis. In the piers, the force for the linear analysis had more than double the force and nearly three times the displacement of the nonlinear analysis. Similar findings can be seen for 090 Fortuna. This high variance may be attributed to the fact that these records had the highest forces and displacement in all of the categories. Higher ground motion intensity, characterized by Fortuna and El Centro, appear to have more variance in displacements and forces between nonlinear and linear analyses than lower intensity ground motions.

Most of the displacement and force occurat the piers. The analysis' forces at the piers yield much more variance than that of the abutments. However, the linear analysis displacements and forces are not too far off of the nonlinear analysis displacement and forces for abutments. The study suggests that the use of k_{isol} in place of nonlinear bearing properties introduces large uncertainties in the predicted performance. This finding echoes similar studies, such as those by Steelman and Hajjar (2009), which noted that nonlinear static approaches generally provide only an approximate and appreciably uncertain representation of nonlinear dynamic structural behavior. Structural engineers should be aware of and appreciate these limitations in their design processes and expectations for extreme event behavior.

Future Works

This study should be attempted again for the same structure to validate Buckle's benchmark bridge #2. It may also be worthwhile to validate the linear modal analysis with linear direct integration analysis. Unfortunately, this was not able to be completed in this study. Other kinds of bridges should also be studied to see how appropriate model simplifications are for other kinds of bridges. Validating Buckle's benchmark bridge #1, a 3-span, 6 pre-cast continuous girders, 3 columns piers bridge would be a suitable bridge to model and analyze. Furthermore, more complicated kinds of structures could be studied.

A similar study reviewed is a document with the research code: FHWA-ICT-13-015. The study is called "Seismic Performance of Quasi-Isolated Highway Bridges in Illinois" prepared by researchers from the University of Illinois at Urbana-Champaign and published by the Illinois Center for Transportation (LaFave et al., 2013). Dr. Steelman, the faculty advisor for this undergraduate thesis, was a part of this project during his time at Urbana-Champaign. This study looked at the performance of multi-span, continuous steel bridges with concrete superstructures that are simply supported at the abutments. Stub abutments and H pile foundations were used in these models. 48 bridge models were developed using OpenSees software with varying pier types (multi-column vs. wall piers), height of piers, soil stiffnesses, type of foundation (fixed vs. flexible), and type of elastomeric bearings (Type I vs Type II).

The Illinois Center for Transportation defines Type I bearings as "A ductile substructure with essentially elastic superstructure. This is the conventional seismic design approach, and it is representative of the way that many IDOT [Illinois Department of Transportation] bridges are currently designed for seismic effects (p.3)." Type I bearings are elastomeric bearings. Type II bearings are defined as "An essentially elastic substructure with ductile superstructure. This less

common approach applies only to steel superstructures with specially detailed ductile cross-frames." (p.3)" Type III bearings were not studied closely, but are defined as "An elastic superstructure and substructure with a fusing mechanism in between. This approach is characteristic of traditional seismic isolation, and is also generally representative of the philosophy IDOT is targeting with the quasi-isolated ERS concept. (p.3)"

The conclusions that the researchers made are that Type II bearings were more likely to unseating because "…the area of the bearing surface was often insufficient given the magnitude of the displacement demand. (p.59)" Bridges with taller piers were also observed become unseated as well. Type I bearings were found to be much less susceptible to unseating. Bearing unseating is a type of failure that bridges are prone to with high ground movement exerted to it. Unseating happens just above the piers and leads to the superstructure being very unstable and dangerous.

Another similar study is a dissertation called "Seismic Performance Assessment of Quasi-Isolated Highway Bridges with Seat-Type Abutments", by a University of Illinois at Urbana-Champaign researcher, Jie Luo, was reviewed (Luo, 2016). Luo worked to test the seismic performance of prototype quasi-isolated bridges and validate design standards that are in place. The bridge models that were analyzed in this study were three or four-spans with either steel-plate or precast-prestressed-concrete (PPC) girders. They had a concrete deck, sacrificial superstructure-substructure connections, seat-type abutments, and multi-column reinforced-concrete (RC) piers that have steel H-pile foundations beneath them.

Four main types of bridge prototypes were developed: **3**-span **S**teel-plate-girder bridges (**3S**), **4**-span-**S**teel-plate-girder bridges (**4S**), **3**-span precast-prestressed-**C**oncrete-girder bridges (**3C**), and **4**-span precast-prestressed-**C**oncrete-girder bridges (**4C**). The bridge models were

made to reflect typical new designs for earthquake-resistant highway bridges of Illinois. Five skew angles (0°, 15°, 30°, 45°, and 60°), two pier column clear heights (15 ft. and 40 ft.), and two soil conditions (hard and soft soils) were varied in the study to make 20 bridge models per main type of prototype (**3S, 4S, 3C,** or **4C**) for a total of 80 models.

Based on the findings in the FHWA document discussed earlier, Luo only studied the results of the Type I elastomeric bearings since they were found to be less prone to unseating than Type II bearings. Analysis of the finite models were reviewed and Luo found that most of the models exhibited suitable seismic performance, but a few models showed higher risk of limited local damage such as bearing unseating or pier column damage. Fortunately, none of the bridges exhibited the risk of actually collapsing when ground motions were applied to the bridge. Luo observed that models that had a higher risk of bearing unseating were those with highly skewed and tall pier columns. Luo also had a smaller number of models with non-skew or lightly-skewed and short pier columns that had pier column damage.

Luo suggests that engineers "strengthen the bearing side retainers at the abutments of highly skewed bridges supported by tall piers. (p. 303)" Luo also recommends that engineers "weaken the commonly over-designed superstructure-to-fixed-pier connections of non-skew or lightly-skewed bridges with short pier columns, in order to mitigate column damage. (p.303)" During an earthquake, ground motions cause for the piers to move. Short piers are typically stiffer due to their short length which are susceptible to damage when ground motions are applied. Making the superstructure to pier more flexible could allow for damage to be minimized. Reviewing and changing design procedures challenge engineers because stiffness is needed to minimize vibrations while commuters are on the bridge, but flexible enough to not be damaged during seismic activity. Studies like these two should be performed in order to improve

and expand engineers' knowledge of how different bearings perform under different circumstances.

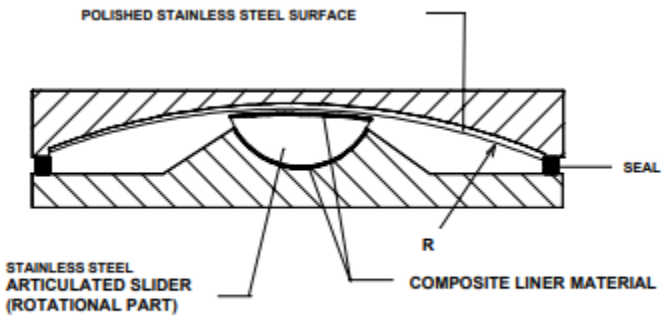

Figure 7. Spherical Friction Bearing

Works Cited

AASHTO (2014), *AASHTO Guide Specifications for Seismic Isolation Design 4th Ed.*, 269-298

AASHTO (2017). *AASHTO LRFD Bridge Design Specifications 6th Ed.*

Ancheta, T. D., Darragh, R. B., Stewart, J. P., Seyhan, E., Silva, W. J., Chiou, B. S. J., Wooddell, K. E., Graves, R. W., Kottke, A. R., Boore, D. M., Kishida, T., and Donahue, J. L. (2013). "PEER NGA-West2 Database."

Buckle, I., Moustafa, A., Monzon, E., (2012). "Annual Meeting AASHTO Subcommittee on Bridges and Structures."

LaFave, J., Fahnestock, L., Foutch, D., Steelman, J.S., Revell, J., Filipov, E. (2013). "Seismic Performance of Quasi-Isolated Highway Bridges in Illinois." *Illinois Center for Transportation (ICT) and Federal Highway Administration (FHA),* 67-70

López-Mosquera, F. (2017). "Hyperelastic Structural Fuses for Improved Earthquake Resilience of Steel Concentrically-Braced Buildings.", 37-41

Luo, J. (2016). "Seismic Performance Assessment of Quasi-Isolated Highway Bridges with Seat-Type Abutments."

Marsh, M. L., Stringer, S. J. (2013). "Performance-Based Seismic Bridge Design.", *National Cooperative Highway Research Program (NCHRP) Synthesis 440*

Mayes, R. L. (2012). "Using Seismic Isolation and Energy Dissipation to Create Earthquake-Resilient Buildings.", *Bulleting of the New Zealand Society for Earthquake Engineering,* 117-122

Steelman, J. S., Hajjar, J. F., "Influence of Inelastic Seismic Response Modeling on Regional Loss Estimation.",